Coordination Chemistry Reviews 254 (2010) 1260–1272

Contents lists available at ScienceDirect

Coordination Chemistry Reviews

journal homepage: www.elsevier.com/locate/ccr

Review

Construction of M–M bonds in late transition metal complexes

Xia Meng, Fusong Wang, Guo-Xin Jin*

Shanghai Key Laboratory of Molecular Catalysis and Innovative Material, Department of Chemistry, Fudan University, Handan Road 220, Shanghai, 200433, PR China

Contents

1. Introduction ... 1260
2. Construction of multinuclear complexes ... 1261
  2.1. General strategy ... 1261
  2.2. Binuclear complexes with metal–metal bonds ... 1261
    2.2.1. Formation of Co–Co, Rh–Rh, Ir–Ir, Ru–Ru homonuclear bonds ... 1261
    2.2.2. Formation of Ru–Co/Rh/Ir bonds ... 1265
    2.2.3. Formation of Rh–Co/Ir bonds ... 1266
    2.2.4. Formation of Rh/Co-Mo/W bonds ... 1268
    2.2.5. Formation of Co/Rh/Ir–Fe bonds ... 1268
  2.3. Trinuclear complexes with metal–metal bonds ... 1268
    2.3.1. Formation of M–Mo/W–M (M = Co, Rh, Ir) bonds ... 1268
    2.3.2. Formation of M–Ni–M (M = Co, Rh) bonds ... 1268
    2.3.3. Formation of M–Co–Co (M = Co, Rh, Ir) bonds ... 1269
    2.3.4. Homo- and hetero-metallic tri- and tetra-nuclear complexes with Ir, Rh and Ru ... 1270
3. Applications of multimetallic clusters ... 1271
4. Conclusion ... 1272
  Acknowledgments ... 1272
  References ... 1272

ARTICLE INFO

Article history:
Received 26 March 2009
Accepted 4 July 2009
Available online 16 July 2009

Keywords:
Metal–metal bonds
Half-sandwich complexes
Carborane
Chalcogenolate ligands
Molecular structures

ABSTRACT

The 16-electron Co, Rh and Ir half-sandwich complexes of $Cp^{\#}M[E_2C_2(B_{10}H_{10})]$ and $Cp^{\#}M(E_2S_2C_6H_4)$ (M = Co, Rh, Ir, Ru; E = S, Se) containing chelating 1,2-dicarba-*closo*-dodecaborane-1,2-dichalcogenolato ligands and benzenedithiolato ligands are promising precursors to build multimetallic clusters by reactions with low oxidation state late transition metal reagents. Such reactions lead to successful constructions of M–M bonds between iridium, rhodium, cobalt, ruthenium, and other late transition metals. Most of these complexes have been characterized by X-ray single crystal determinations and some have been studied by computational methods. Such theoretical studies reveal the covalent bonding nature of those multinuclear complexes. Some of these clusters have been found to have interesting nonlinear optical properties.

1. Introduction

The discovery and intensive study of M–M bonds between transition metal atoms can be traced back approximately a century. Thus many multimetallic clusters containing direct M–M interactions are now well known and have numerous applications. [1a–e]. Classical examples of metal–metal bonded species such as $Hg_2(NO_3)_2$, $Fe_2(CO)_9$, W_2Cl_9, $[Cp(CO)_3Mo]_2$ and $[Re_2Cl_8]^{2-}$ have been extensively investigated. At the same time, theories discussing the formation and construction of single and multiple metal–metal bonds are well developed. Generally speaking, the overlap of d orbitals leads to different types of covalent M–M bonding interactions and the extra stabilization energy gained from the rearrangement of d electrons is considered to be the driving force for M–M bond formation. In the past few decades, developments of X-ray single crystal determination methods as well as density functional theory gave new vitality to this field. A large numbers of multimetallic complexes have been synthesized and well characterized [1]. Up to now, several strategies have been widely used in the formation of bonds between late transition metals,

---

* Corresponding author. Tel.: +86 21 65643776; fax: +86 21 65643776.
E-mail address: gxjin@fudan.edu.cn (G.-X. Jin).

0010-8545/$ – see front matter © 2009 Elsevier B.V. All rights reserved.
doi:10.1016/j.ccr.2009.07.002

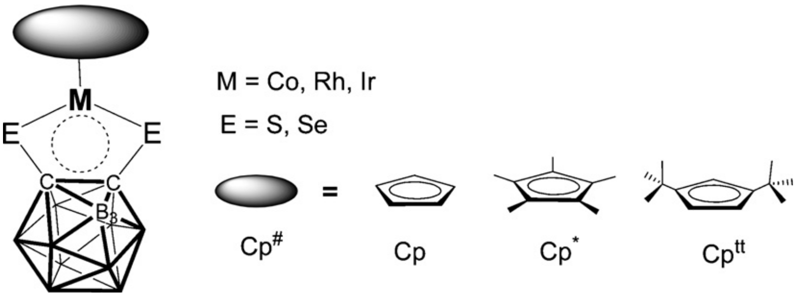

Fig. 1. 16-Electron half-sandwich precursor $\mathrm{Cp^{\#}M[E_2C_2(B_{10}H_{10})]}$.

including metal exchange reactions from multimetallic hydrides, halides and other salts supported by carbonyl and cyclopentadienyl groups; condensation reactions with mononuclear species; and photochemical strategies [2]. In most cases, efficient ancillary ligands such as chloride, carbon monoxide and cyclopentadienyl derivatives are involved, supporting and stabilizing the M–M bonds between transition metals [1].

During the past decade 1,2-dicarba-*closo*-dodecarborane-1,2-dichalcogenolates have been synthesized and used as ligands in the construction of multinuclear organometallic clusters successively. In a previous review, the main reaction patterns of those ligands were discussed and various multinuclear complexes were reported [1f]. This review discusses a systematic strategy for the construction of heterometallic covalent bonds between different metals, including some simple theoretical analysis, as well as some applications as nonlinear optical materials.

Shortly after the discovery of 1,2-dicarba-*closo*-dodecarborane-1,2-dichalcogenolates, the coordination chemistry of their 16-electron "*pseudo*-aromatic" half-sandwich complexes $\mathrm{Cp^{\#}M[E_2C_2(B_{10}H_{10})]}$ ($\mathrm{Cp^{\#}} = \eta^5$-cyclopentadienyl derivatives; M = Co, Rh, Ir; E = S, Se, Fig. 1) began to receive considerable attention [2–6]. The free 1,2-dichalcogenolates can be easily prepared by the insertion of elemental chalcogen into the Li–C bonds of dilithium carborane obtained by deprotonation of carborane by *n*-butyl lithium [4]. The metal half-sandwich complexes have been well documented to have high stability as well as multiple active sites on the transition metal centers, the sulfur or selenium atoms, and the B3/B6 boron atoms. Their chemical reactivity makes them promising precursors for the construction of multinuclear complexes containing M–M bonds [1f].

Several structural and electronic advantages have been considered when exploring the syntheses of these multinuclear complexes. Firstly, a 16-electron unsaturated metal center is susceptible towards nucleophilic attack, which has been well confirmed by direct insertions of mono-, bi-, tri- and tetra-dentate ligands [1g]. Secondly, the sulfur or selenium atoms can function as good bridging or chelating donors owing to their filled p_z orbitals as indicated by DFT calculations. A typical example is $\mathrm{Cp^{*}Ir[S_2C_2(B_{10}H_{10})]}$, which demonstrates strong bonding and B–H activation tendencies. Its HOMO is mainly localized on the iridium and sulfur atoms (Fig. 2). The extraordinary big contribution of the sulfur p_z orbital makes it susceptible towards nucleophilic attack during the formation of metal–metal bonds when it becomes a bridging ligand. Meanwhile, the big contributions of p_z and d orbitals from iridium in the empty LOMO ensure the facile nucleophilic attack from the electron-rich low-oxidation-state reagents. Natural population analysis shows higher positive charges on B3 and B6 than on the other carborane boron atoms by factors of 2–20, thereby suggesting that they are more susceptible towards external attack. This also provides a good explanation for the increased tendency for B–H activation in the two positions. Thirdly, the shielding by the carboranyl cage and the bulky cyclopentadienyl ligand is expected to increase the stability of both the precursors and target multinuclear complexes, and at the same time make them more soluble and readily crystallized. The 16-electron precursors of $\mathrm{Cp^{\#}M(E_2C_6H_4)}$ also demonstrate similar electronic advantages [7–11]. Several multimetallic clusters containing direct M–M bonds have been obtained using this strategy.

2. Construction of multinuclear complexes

2.1. General strategy

Half-sandwich late transition metal complexes of the types $\mathrm{Cp^{\#}M[E_2C_2(B_{10}H_{10})]}$ and $\mathrm{Cp^{\#}M(E_2S_2C_6H_4)}$ are the important starting materials in most cases and almost all of the reactions are based on the direct combination of these precursors with other metal reagents. The general approach of combining them with low oxidation state electron-rich metal complexes such as $\mathrm{[M(COD)(\mu\text{-}Cl)]_2}$ (COD = 1,5-cyclooctadiene) and $\mathrm{[M(CO)_2(\mu\text{-}Cl)]_2}$ (M = Rh, Ir, Ru) was found to be very successful thus taking advantage of the electron deficiency on the metal center and the strong assisting potential of the ancillary ligands. The metal centers undergo redox reactions leading to polar bonds between different metal centers. A series of homo- and hetero- bi-, tri- and tetra-nuclear complexes have been synthesized exhibiting diverse structures and bonding situations (Table 1). Most of these complexes have been fully characterized by IR, NMR, elemental analysis and X-ray single crystal structure determinations. Herein, we develop this strategy into a systematic methodology for the facile formation of covalent metal–metal bonds, seeking a comprehensive understanding of their chemistry and underlying properties.

2.2. Binuclear complexes with metal–metal bonds

2.2.1. Formation of Co–Co, Rh–Rh, Ir–Ir, Ru–Ru homonuclear bonds

Homo-bimetallic complexes with covalent M–M bonds can be prepared by two methods. (1) Directly as byproducts from the syntheses of 16-electron mononuclear half-sandwich carboranyl complexes of Co, Rh, Ir and Ru [5,6] and (2) reactions of the 16-

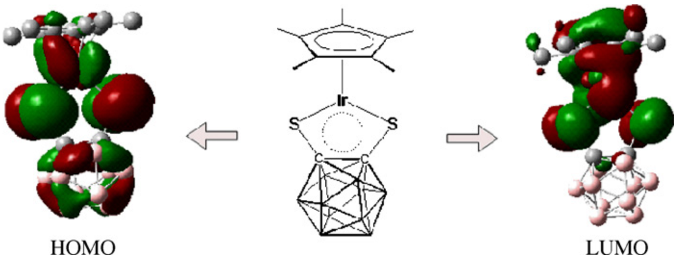

Fig. 2. Frontier orbitals of the 16-electron iridium complex.

Table 1
Selected complexes with M–M bonds ($Cp^{*} = \eta^5$-pentamethylcyclopentadienyl, $Cp^{tt} = \eta^5$-1,3-ditert-butylclopentadienyl, $Cp = \eta^5$-cyclopentadienyl, COD = 1,5-cyclo-octadiene).

M–M′	Bond length (Å)		Complexes		References
Ir–Ir	2.6924(8)		**3b**	$(Cp^{*}Ir)_2[Se_2C_2(B_{10}H_{10})]$	[16]
	2.7508(9)		**11a**	$[(COD)Ir](Cp^{*}Ir)(\mu\text{-}OCH_3)[S_2C_2(B_9H_8)]$	[15]
	2.9921(9)		**12a**	$[(COD)Ir](Cp^{*}Ir)[S_2C_2(B_{10}H_9)]$	[15]
	2.7378(8)		**13a**	$[(COD)Ir]_2(\mu\text{-}OCH_3)Cl[S_2C_2(B_9H_9)]$	[15]
	2.8086(13)		**13b**	$[(COD)Ir]_2(\mu\text{-}OCH_3)Cl[Se_2C_2(B_9H_9)]$	[15]
	2.9473(10)	Ir1–Ir2	**14b**	$[(COD)Ir]_2[S_2C_2(Ir(C_8H_{13})B_9H_8(\mu\text{-}OCH_3)]$	[15]
	3.0866(10)	Ir2–Ir3			
	2.8928(16)		**15a**	$[(COD)Ir]_2[S_2C_2(B_{10}H_8)(OCH_3)_2]$	[15]
	2.8939(15)		**15b**	$[(COD)Ir]_2[Se_2C_2(B_{10}H_8)(OCH_3)_2]$	[15]
	2.8608(11)		**16a**	$[(COD)Ir]_2[S_2C_2(B_{10}H_{10})]$	[23]
	2.9126(11)	Ir1–Ir2	**71b**	*cis*-$\{Cp^{*}Ir[Se_2C_2(B_{10}H_{10})]\}\text{-}\{Cp^{*}Ir(OCH_3)[Se_2C_2(B_{10}H_8)]\}Ir$	[27]
	3.1316(13)	Ir2–Ir3			
	2.7276(12)	Ir1–Ir2	**70b**	*trans*-$\{Cp^{*}Ir[Se_2C_2(B_{10}H_{10})]\}\text{-}\{Cp^{*}Ir(OCH_3)[Se_2C_2(B_{10}H_9)]\}Ir$	[27]
	3.1742(15)	Ir2–Ir3			
Ir–Rh	3.0596(12)		**28a**	$Cp^{*}Ir[(COD)Rh][S_2C_2(B_{10}H_9)]$	[15]
	2.7829(10)		**29a**	$Cp^{*}Ir[(COD)Rh][S_2C_2(B_{10}H_{10})]$	[15]
	2.7526(8)		**30a**	$Cp^{*}Ir[(COD)Rh](\mu\text{-}OCH_3)[S_2C_2(B_9H_9)]$	[15]
	2.5983(11)		**31a**	$Cp^{*}Ir[CpRh][S_2C_2(B_{10}H_{10})]$	[14]
	2.6405(11)		**31b**	$Cp^{*}Ir[CpRh][Se_2C_2(B_{10}H_{10})]$	[14]
	2.6630(11)	Ir1–Rh	**74b**	$\{Cp^{*}Rh[Se_2C_2(B_{10}H_{10})]\}_2Ir$	[25]
	2.7097(11)	Ir2–Rh			
	3.003(3)	Ir1–Rh	**72a**	$\{Cp^{*}Ir[S_2C_2(B_{10}H_{10})]\}\{Cp^{*}Ir(\mu\text{-}OCH_3)\text{-}[S_2C_2(B_{10}H_8)]\}Rh$	[25]
	2.685(3)	Ir2–Rh			
	3.074(3)	Ir1–Rh	**72b**	$\{Cp^{*}Ir[S_2C_2(B_{10}H_{10})]\}\{Cp^{*}Ir(\mu\text{-}OCH_3)\text{-}[S_2C_2(B_{10}H_8)]\}Rh$	[25]
	2.663(3)	Ir2–Rh			
	2.5990(10)	Ir1–Rh2	**73a**	$\{(Cp^{*}Ir)_2Rh[(COD)Rh][S_2C_2(B_{10}H_{10})]\text{-}[S_2C_2(B_{10}H_9)]$	[28]
	2.5990(10)	Ir2–Rh1			
	2.9814(10)	Ir2–Rh2			
	2.6281(12)	Ir1–Rh2	**73b**	$\{(Cp^{*}Ir)_2Rh[(COD)Rh][Se_2C_2(B_{10}H_{10})]\text{-}[Se_2C_2(B_{10}H_9)]$	[28]
	2.8258(13)	Ir2–Rh1			
	3.0085(13)	Ir2–Rh2			
Ir–Co	2.5967(11)	Ir–Co1	**63a**	$Cp^{*}Ir[S_2C_2(B_{10}H_{10})][Co_2(CO)_5]$	[22]
	2.6244(11)	Ir–Co2			
	2.6156(13)	Ir–Co1	**63b**	$Cp^{*}Ir[Se_2C_2(B_{10}H_{10})][Co_2(CO)_5]$	[22]
	2.6460(13)	Ir–Co2			
	2.5974(9)	Ir–Co1	**65a**	$\{Cp^{*}Ir(S_2C_6H_4)\}Co_2(CO)_5$	[10]
	2.6122(9)	Ir–Co2			
Ir–Ru	2.7064(6)	Ir1–Ru	**75a**	$\{Cp^{*}Ru[S_2C_2(B_{10}H_{10})]\}_2Ir$	
	2.7136(6)	Ir2–Ru			
	2.7639(6)		**20a**	$Cp^{*}Ir[(COD)Ru][S_2C_2(B_9H_8)(H)]$	[17]
	2.7593(16)		**23a**	$Cp^{*}Ir[(COD)Ru](OCH_3)[S_2C_2(B_9H_8)]$	[17]
	2.7064(6)	Ir1–Ru	**75a**	$\{Cp^{*}Ru[S_2C_2(B_{10}H_{10})]\}_2Ir$	
	2.7136(6)	Ir2–Ru			
Rh–Rh	2.6245(9)		**2a**	$(Cp^{*}Rh)_2[S_2C_2(B_{10}H_{10})]$	[20]
	2.6686(17)		**2b**	$(Cp^{*}Rh)_2[Se_2C_2(B_{10}H_{10})]$	[20]
	2.8809(11)		**4a**	$[(COD)Rh]_2[S_2C_2(B_{10}H_{10})]$	[12]
	2.935(3)		**4b**	$[(COD)Rh]_2[Se_2C_2(B_{10}H_{10})]$	[12]
	2.8900(11)		**5a**	$[(CO)_2Rh]_2[S_2C_2(B_{10}H_{10})]$	[12]
	2.5627(10)		**9a**	$(CpRh)_2[S_2C_2(B_{10}H_{10})]$	[14]
	2.5721(8)		**10a**	$(CpRh)(Cp^{*}Rh)[S_2C_2(B_{10}H_{10})]$	[14]
	2.6112(10)		**10b**	$(CpRh)(Cp^{*}Rh)[Se_2C_2(B_{10}H_{10})]$	[14]
	2.6460(7)	Rh1–Rh2	**68a**	*cis*-$\{Cp^{*}Rh[S_2C_2(B_{10}H_{10})]\}_2Rh$	[26]
	2.6460(7)	Rh2–Rh3			
	2.8232(11)	Rh1–Rh2	**69a**	*trans*-$\{Cp^{*}Rh[S_2C_2(B_{10}H_{10})]\}_2Rh$	[26]
	2.8232(11)	Rh2–Rh3			
	2.6588(9)	Rh1–Rh2	**69b**	$(Cp^{*}Rh)_2Rh_2(CO)[Se_2C_2(B_{10}H_{10}]_3$	
	2.6588(9)	Rh1a–Rh2a			
	2.6784(13)	Rh2–Rh2a			

Table 1 (*Continued*)

M–M′	Bond length (Å)		Complexes		References
Rh–Co	2.7057(12)		**25b**	$Cp^*Rh[(COD)Co][Se_2C_2(B_{10}H_{10})]$	[18]
	2.6177(17)		**26a**	$Cp^*Rh[(COD)Co][S_2C_2(B_{10}H_{10})]$	[18]
	2.4778(11)		**27a**	$Cp^*Rh[CpCo][S_2C_2(B_{10}H_{10})]$	[14]
	2.5092(16)		**27b**	$Cp^*Rh(CpCo)[Se_2C_2(B_{10}H_{10})]$	[14]
	2.6057(9	Rh–Co1	**61a**	$Cp^*Rh[S_2C_2(B_{10}H_{10})][Co_2(CO)_5]$	[20]
	2.6399(9)	Rh–Co2			
	2.6197(9)	Rh–Co1	**61b**	$Cp^*Rh[Se_2C_2(B_{10}H_{10})][Co_2(CO)_5]$	[20]
	2.6583(9)	Rh–Co2			
	2.5957(12)	Rh–Co1	**66a**	$\{Cp^*Rh(S_2C_6H_4)\}Co_2(CO)_5$	[10]
	2.6079(11)	Rh–Co2			
Rh–Ru	2.7261(9)		**18a**	$Cp^*Rh[(COD)Ru][S_2C_2(B_{10}H_9)(\mu\text{-}H)]$	[17]
	2.7498(9)		**19a**	$Cp^*Rh[(COD)Ru][S_2C_2(B_9H_8)(\mu\text{-}H)]$	[17]
	2.7941(11)		**22b**	$Cp^*Rh[(COD)Ru](\mu\text{-}OCH_3)[Se_2C_2(B_9H_8)]$	[17]
Co–Co	2.5501(10)	Co1–Co3	**59a**	$CpCo[S_2C_2(B_{10}H_{10})][Co_2(CO)_5]$	[23]
	2.5881(10)	Co1–Co2			
	2.4436(10)	Co2–Co3			
	2.4465(11)		**61a**	$Cp^*Rh[S_2C_2(B_{10}H_{10})][Co_2(CO)_5]$	[20]
	2.4478(11)		**61b**	$Cp^*Rh[Se_2C_2(B_{10}H_{10})][Co_2(CO)_5]$	[20]
	2.4452(12)		**63a**	$Cp^*Ir[S_2C_2(B_{10}H_{10})][Co_2(CO)_5]$	[22]
	2.4445(16)		**63b**	$Cp^*Ir[Se_2C_2(B_{10}H_{10})][Co_2(CO)_5]$	[22]
	2.4493(11)		**65a**	$\{Cp^*Ir(S_2C_6H_4)\}Co_2(CO)_5$	[10]
	2.4445(15)		**66a**	$\{Cp^*Rh(S_2C_6H_4)\}Co_2(CO)_5$	[10]
	2.4672(10)		**67a**	$\{Cp^*Ru(S_2C_6H_4)\}Co_2(CO)_5$	[10]
Co–Ru	2.6143(7)	Ru–Co1	**67a**	$\{Cp^*Ru(S_2C_6H_4)\}Co_2(CO)_5$	[10]
	2.6249(10)	Ru–Co			
W–Ir	2.7445(7)	Ir1–W	**53a**	$\{Cp^*Ir_2[S_2C_2(B_{10}H_{10})]_2\}W(CO)_2$	[26]
	2.7851(6)	Ir2–W			
	2.7704(9)	Ir1–W	**53b**	$\{Cp^*Ir_2[Se_2C_2(B_{10}H_{10})]_2\}W(CO)_2$	[26]
	2.8081(8)	Ir2–W			
W–Rh	2.7408(14)		**37a**	$\{Cp^*Rh[S_2C_2(B_{10}H_{10})]\}\{W(CO)_2[S_2C_2(B_{10}H_{10})]\}$	[19]
	2.7458(7)		**39a**	$\{Cp^{tt}Rh[S_2C_2(B_{10}H_{10})]\}\{W(CO)_2[S_2C_2(B_{10}H_{10})]\}$	[19]
	2.7461(16)	Rh1–W	**51a**	$\{Cp^*Rh_2[S_2C_2(B_{10}H_{10})]_2\}W(CO)_2$	[20]
	2.7891(14)	Rh2–W			
	2.7517(12)	Rh1–W	**51b**	$\{Cp^*Rh_2[Se_2C_2(B_{10}H_{10})]_2\}W(CO)_2$	[20]
	2.7517(12)	Rh2–W			
W–Co	2.648(2)		**33a**	$\{Cp^*Co[S_2C_2(B_{10}H_{10})]\}\{W(CO)_2[S_2C_2(B_{10}H_{10})]\}$	[16]
	2.6875(16)		**33b**	$\{Cp^*Co[Se_2C_2(B_{10}H_{10})]\}\{W(CO)_2[Se_2C_2(B_{10}H_{10})]\}$	[16]
	2.6227(13)		**35a**	$\{CpCo[S_2C_2(B_{10}H_{10})]\}\{W(CO)_2[S_2C_2(B_{10}H_{10})]\}$	[16]
	2.626(3)		**40b**	$\{CpCo(Se_2C_6H_4)\}(Se_2C_6H_4)W(CO)_2$	[28]
	2.581(1)	Co1–W	**55a**	$\{CpCo_2[S_2C_2(B_{10}H_{10})]_2\}W(CO)_2$	[28]
	2.581(1)	Co2–W			
Mo–Ir	2.7622(16)	Ir1–Mo	**52a**	$\{Cp^*Ir_2[S_2C_2(B_{10}H_{10})]_2\}Mo(CO)_2$	[25]
	2.7639(18)	Ir2–Mo			
	2.7593(9)	Ir1–Mo	**52b**	$\{Cp^*Ir_2[Se_2C_2(B_{10}H_{10})]_2\}Mo(CO)_2$	[25]
	2.7593(9)	Ir2–Mo			
Mo–Rh	2.7403(17)		**36a**	$\{Cp^*Rh[S_2C_2(B_{10}H_{10})]\}\{Mo(CO)_2[S_2C_2(B_{10}H_{10})]\}$	[19]
	2.754(2)	Rh1–Mo	**49a**	$\{Cp^*Rh_2[S_2C_2(B_{10}H_{10})]_2\}Mo(CO)_2$	[19]
	2.803(2)	Rh2–Mo			
	2.7839(11)	Rh1–Mo	**49b**	$\{Cp^*Rh_2[Se_2C_2(B_{10}H_{10})]_2\}Mo(CO)_2$	[19]
	2.8253(10)	Rh2–Mo			
	2.7705(13)	Rh1–Mo	**50a**	$\{Cp^{tt}Rh_2[S_2C_2(B_{10}H_{10})]_2\}Mo(CO)_2$	[24]
	2.7705(13)	Rh2–Mo			
	2.798(3)	Rh1–Mo	**50b**	$\{Cp^{tt}Rh_2[Se_2C_2(B_{10}H_{10})]_2\}Mo(CO)_2$	[24]
	2.803(3)	Rh2–Mo			
	2.7184(7)	Rh1–Mo	**56a**	$\{CpRh(S_2C_6H_4)\}_2Mo(CO)_2$	[9]
	2.7621(7)	Rh2–Mo			

Table 1 (*Continued*)

M–M′	Bond length (Å)		Complexes		References
Mo–Co	2.5001(9)		**32a**	$\{Cp^*Co[S_2C_2(B_{10}H_{10})]\}\{Mo(CO)_2[S_2C_2(B_{10}H_{10})]\}$	[23]
	2.724(2)		**32b**	$\{Cp^*Co[Se_2C_2(B_{10}H_{10})]\}\{Mo(CO)_2[Se_2C_2(B_{10}H_{10})]\}$	[23]
	2.6264(8)	Co1–Mo	**48a**	$\{CpCo_2[S_2C_2(B_{10}H_{10})]_2\}Mo(CO)_2$	[23]
	2.6264(8)	Co2–Mo			
	2.6182(8)	Co1–Mo	**54a**	$\{CpCo(S_2C_6H_4)\}_2Mo(CO)_2$	[7]
	2.6327(9)	Co2–Mo			
	2.633(1)	Co1–Mo	**54b**	$\{CpCo(Se_2C_6H_4)\}_2Mo(CO)_2$	[7]
	2.641(1)	Co2–Mo			
Fe–Ir	2.5762(11)		**46b**	$\{Cp^*Ir[Se_2C_2(B_{10}H_{10})]\}Fe(CO)_3$	[22]
Fe–Rh	2.5143(8)		**44a**	$\{Cp^*Rh[S_2C_2(B_{10}H_{10})]\}Fe(CO)_3$	[21]
	2.5500(11)		**45b**	$\{Cp^*Rh[Se_2C_2(B_{10}H_{10})]\}Fe(CO)_3$	[21]
	2.5128(14)		**45a**	$\{Cp^{tt}Rh[S_2C_2(B_{10}H_{10})]\}Fe(CO)_3$	[21]
Fe–Co	2.398(14)		**41a**	$\{CpCo[S_2C_2(B_{10}H_{10})]\}Fe(CO)_3$	[21]
	2.4227(10)		**42a**	$\{Cp^*Co[S_2C_2(B_{10}H_{10})]\}Fe(CO)_3$	[21]
	2.420(1)		**47a**	$[CoCp(S_2C_6H_4)]$	[7]
Ni–Rh	2.458(6)	Rh1–Ni	**54a**	$\{CpRh[S_2C_2(B_{10}H_{10})]\}_2Ni$	[24]
	2.458(6)	Rh2–Ni			
	2.4921(15)	Rh1–Ni	**54b**	$\{CpRh[Se_2C_2(B_{10}H_{10})]\}_2Ni$	[24]
	2.4921(15)	Rh2–Ni			
Ni–Co	2.3644(15)	Co1–Ni	**53a**	$\{CpCo[S_2C_2(B_{10}H_{10})]\}_2Ni$	[23]
	2.3710(17)	Co2–Ni			

electron complexes with low oxidation state complexes such as half-sandwich carbonyl reagents, ethylene reagents, and COD functionalized reagents [12].

Binuclear Co–Co, Rh–Rh and Ir–Ir complexes containing a $[C_2E_2(B_{10}H_{10})]^{2-}$ bridging ligand are obtained in relatively low yield (<20%) from the reactions of chalcogen-inserted dilithium carborane with the corresponding half-sandwich cobalt, iridium and rhodium complexes (**1a/b**–**3a/b**) (Scheme 1). In the highly symmetrical homo-binuclear complex, dithiolato carborane serves as a bridging ligand. Each metal center is also connected to a cyclopentadienyl ligand. The distances between the two metals are 2.62 Å (**2a**) and 2.69 Å (**3a**) respectively, in the range of M–M single bonds. Binuclear low oxidation state Rh complexes are prepared using similar precursors. Thus reactions of dimeric $[Rh(COD)(\mu\text{-}Cl)]_2$ (COD = 1,5-cyclo-octadiene, C_8H_{12}) or $[Rh(CO)_2(\mu\text{-}Cl)]_2$ with $Li_2E_2C_2B_{10}H_{10}$ give the complexes $(LRh)_2[E_2C_2(B_{10}H_{10})]$ (L = COD, **4a**, **4b**; L = 2CO, **5a**, **5b**) at room temperature. As for ruthenium, reaction of $[C_2S_2(B_{10}H_{10})]^{2-}$ with the 17-electron fragment $[CpRu(PPh_3)_2]$ or $[Cp^*RuCl(\mu\text{-}Cl)]_2$ gives a symmetric bimetallic complex $(CpRu)_2[S_2C_2(B_{10}H_{10})]_2$ (**7a**) as the main product with a Ru–Ru distance is 2.78 Å, also corresponding to a single bond [5]. Another approach uses 1,2-dicarba-*closo*-dodecarborane directly as bidentate ligand. For example, the air- and water-sensitive binuclear rhodium complex $(Cp^*Ru)_2(\mu\text{-}Cl)(\mu\text{-}H)[S_2C_2(B_{10}H_{10})]_2$ (**6**) is obtained from the reaction of $(B_{10}H_{10})C_2S_2Li_2$ with $[Cp^*Rh(\mu\text{-}Cl)_2]_2$. The resonance at δ −15.19 ppm in the ^1H NMR implies the existence of a bridging H atom accompanying the bridging chloride atom. According to the X-ray crystal determination, the Rh–Rh distance is 2.82 Å, which is longer than that in **2a**, **2b**, **4a**, **4b** and **5a**, **5b** [12].

The other synthetic method uses half-sandwich precursors to construct M–M bonds. Extensive explorations reveal that M–M bonds between group 9 metals can be constructed by well designed reactions of the 16-electron complex $Cp^{\#}M[E_2C_2(B_{10}H_{10})]$ with low oxidation state transition metal complexes (Scheme 2). This facile synthetic approach has already been used successfully for the formation of the homo-binuclear Co–Co complex (**1a**) by Kang as early as 1999 [13]. The analogous complexes with Rh–Rh bonds can be obtained from $[(COD)Rh(\mu\text{-}Cl)]_2$. Three different types of complexes are isolated from the reaction mixtures, namely symmetric binuclear complexes containing $(Cp^*Rh)_2$ fragments (**2a**, **2b**), binuclear complexes containing $[(COD)Rh]_2$ fragments (**4a**, **4b**) and asymmetric complexes $(Cp^*Ru)(CODRu)(\mu\text{-}Cl)[E_2C_2(B_{10}H_{10})]_2$ without any metal–metal interaction as indicated by a Rh–Rh distance of 3.38 Å (**8a**, **8b**). Similar reactions of $CpRhL_2$ (L = CO, C_2H_4) with $Cp^{\#}Rh[S_2C_2(B_{10}H_{10})]$ afford complexes **9a** and **10a** with Rh–Rh distances of 2.56 Å (for **9a**) and 2.57 Å (for **10a**) [14]. Apparently in all of these rhodium complexes, the rhodium fragments of the original carborane precursors have been reduced from Rh^{III} to Rh^{II} by $CpCo(C_2H_4)_2$, $CpRh(L)_2$ and $[(COD)Rh(\mu\text{-}Cl)]_2$.

Use of similar methods for the syntheses of Ir–Ir complexes does not give a satisfactory result owing to the complexity of the reactions. However, studies using different solvents and reaction conditions demonstrate more fascinating chemistry of these di-iridium complexes (Scheme 3). Thus a number of homo-bimetallic iridium complexes with B–H activations, B–B cleavages or Ir–B interactions have been isolated after heating 16-electron half-sandwich iridium precursors with 1 equiv. of $[Ir(COD)(\mu\text{-}OCH_3)]_2$ or 4 equiv. of $[Ir(COD)(\mu\text{-}Cl)]_2$ in the presence of MeOH (**11a/b**–**15a/b**) (Fig. 1). For example, $[(COD)Ir](Cp^*Ir)(\mu\text{-}OCH_3)[E_2C_2(B_9H_8)]$ (**11a**, **11b)** and $[(COD)Ir]_2(\mu\text{-}OCH_3)Cl[E_2C_2(B_9H_9)]$ (**13a**, **13b)** are Ir–Ir-*nido*-carborane products in which Cp^*Ir and (COD)Ir fragments are bridged by two S or Se atoms that are linked to the open C_2B_3 face. The metal, bonded by an O atom connected to B3 as a result of B–H activation, are arranged at one side of the cup-shaped *nido*-carborane like a cup handle. In all of these complexes, the presence of Ir–B bonds and methoxy substituted carboranes indicates the activation of B(3)–H and B(6)–H. The unexpected products $[(COD)Ir]_2(\mu\text{-}OCH_3)$ $[S_2C_2(Ir(C_8H_{13})B_9H_8]$ (**14a**, **14b**) in which the third iridium atoms replaces B3 are isolated in the same reactions. The bond length between Ir1 and Ir2 is 2.95 Å, while the Ir2 and Ir3 distance is lengthened to 3.09 Å [15]. Compared with the similar reactions of cobalt, rhodium and ruthenium complexes, almost all the iridium counterparts demonstrate strong tendency of B–B, B–H activation and the products seem to be more complicated and uncontrollable. It could be explained as the radial and coordina-

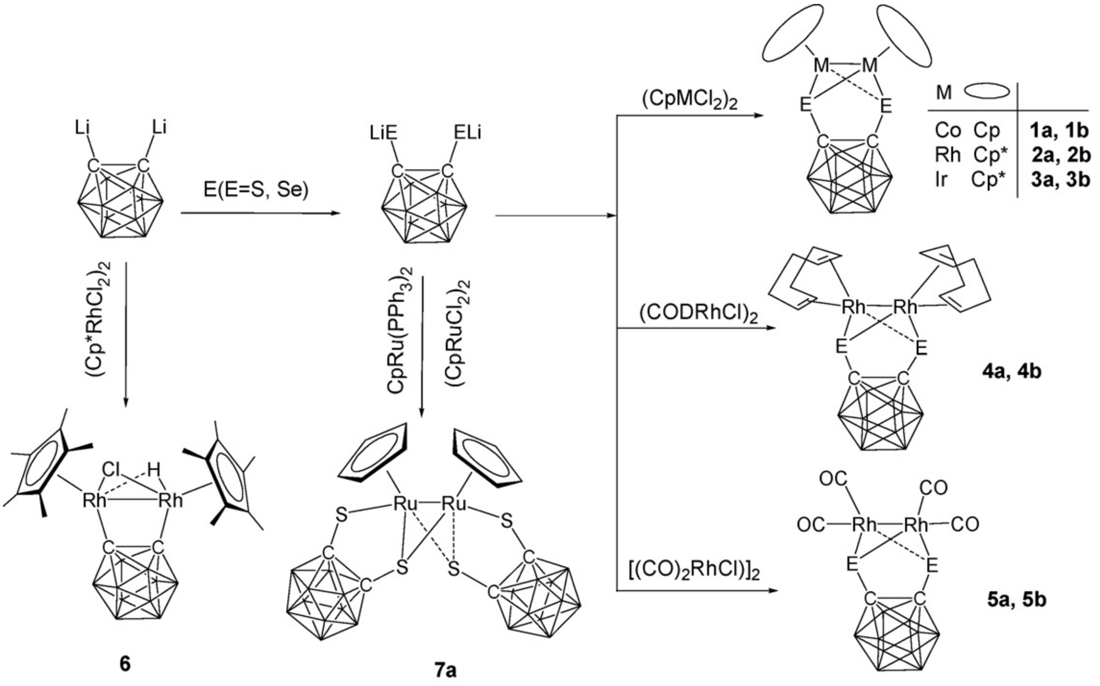

Scheme 1. Syntheses of binuclear complexes from lithium salts of 1,2-dicarba-*closo*-dodecarborane.

tive flexibilities of the iridium atoms. In addition, the complexes are stabilized by Ir–B interactions.

Beside the intentional design of the homo-binuclear complexes, complexes containing Rh–Rh and Ir–Ir singlet bonds are also observed in many reactions as byproducts. For example, in the preparation of binuclear Co–Rh complexes, Ir–Rh complexes, and trinuclear Rh–Mo/W–Rh complexes, the homo-binuclear complexes **2a** and **2b** are always isolated in low yield. Furthermore, the reaction of CpCo[$E_2C_2(B_{10}H_{10})$] with [(COD)Ir((μ-Cl)]$_2$ affords [(COD)Ir]$_2$[$E_2C_2(B_{10}H_{10})$] (**16a** and **16b**) as the only products, instead of any expected heterometallic complexes [16]. The discovery of the unexpected homo-bimetallic species instead of heterometallic complexes reveal the trends of M–M bonding between the same metals, partially because there are better matching for d orbitals and complexes with higher symmetry are formed.

2.2.2. Formation of Ru–Co/Rh/Ir bonds

In principle, hetero-bimetallic complexes with direct M–M interactions can be synthesized following the same method. How-

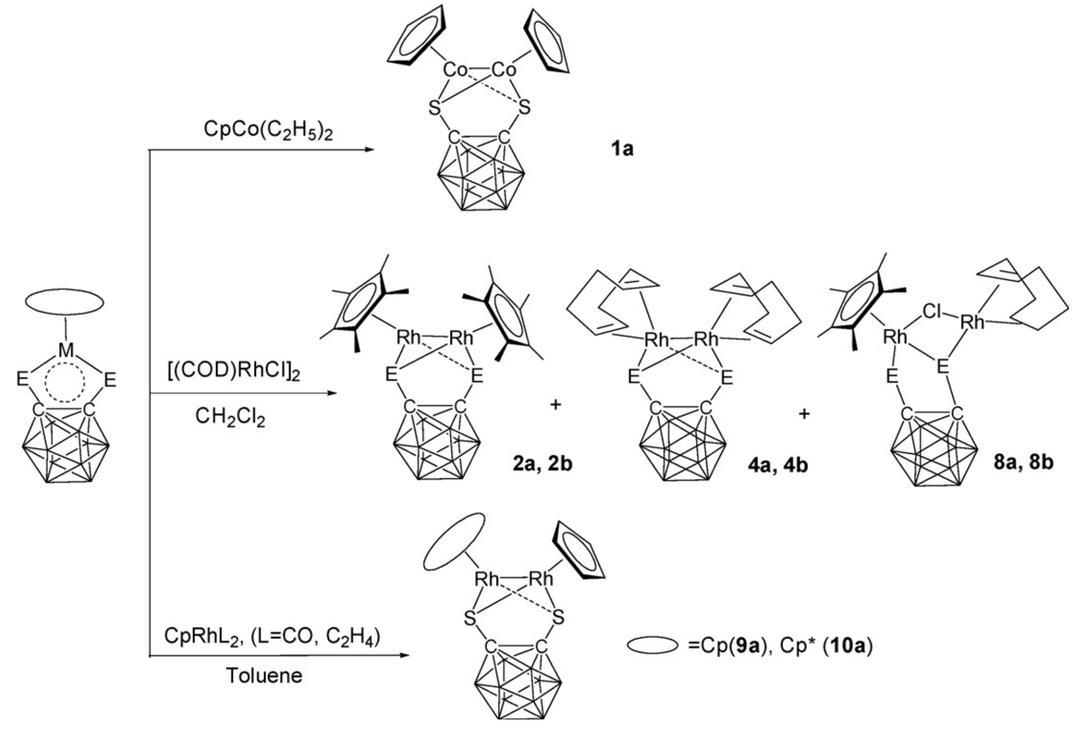

Scheme 2. Syntheses of binuclear Co and Rh complexes from 16-electron precursors.

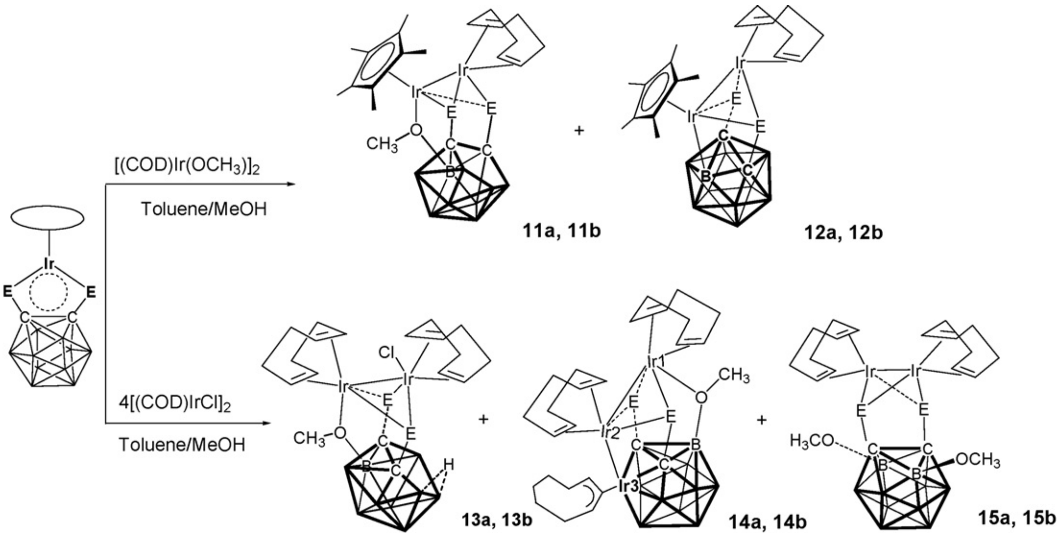

Scheme 3. Syntheses of binuclear Ir complexes from the 16-electron precursor.

ever, not all such reactions lead to the expected results. Some lead to complicated intractable reaction mixtures. Others are too sensitive to be crystallized. Still others some lead to unpredictable products. These systems need further investigation.

Diruthenium complexes with metal–metal bonds are not easy to prepare from reactions of 16-electron precursors with $[(COD)Ru(\mu\text{-}Cl)_2]_x$. In THF, a doubly chloride bridged complex $[Cp^*Rh][(COD)Ru](\mu\text{-}Cl)_2[S_2C_2(B_{10}H_{10})]$ (**17a**) is observed without a direct Rh–Ru bond. Following the previous observations that B–H activation may probably contribute to the stabilization of bimetallic complexes, K_2CO_3 was added as a base to activate the carborane cage. The complex $[Cp^*Rh][(COD)Ru][S_2C_2(B_{10}H_9)(\mu\text{-}H)]$ (**18a**) is obtained with a structure exhibiting a Rh–Ru bond distance of 2.73 Å as well as a calculated Ru–H distance of 2.23 Å, in the range of a metal–hydrogen bond. The use of the weaker base $NaHCO_3$ leads to a series of M–Ru (M = Co, Rh, Ir) hetero-bimetallic complexes $[Cp^*M][(COD)Ru][E_2C_2(B_9H_8)(\mu\text{-}H)]$ (**19a**, **19b**, **20a**, **21a**) and $[Cp^*M][(COD)Ru](\mu\text{-}OCH_3)[E_2C_2(B_9H_8)]$ (**22a**, **22b**, **23a**, **24a**) (Scheme 4). All of these complexes contain open-caged carboranedichalcogenolate ligands with apparent B–H activation. The typical bond lengths in these complexes are 2.75 Å (Rh–Ru, **19a**), 2.76 Å (Ir–Ru, **20a**) and 2.62 Å (Co–Ru, **21a**) [17].

2.2.3. Formation of Rh–Co/Ir bonds

Complexes with Rh–Co bonds are obtained from both 16-electron precursors of ruthenium and cobalt under mild conditions. Reactions of $[Rh(COD)(\mu\text{-}OCH_3)]_2$ or $[Rh(COD)(\mu\text{-}OC_2H_5)]_2$ with $Cp^*Co[Se_2C_2(B_{10}H_{10})]$ in mixed toluene/methanol give an asymmetric selenium-bridged binuclear complex $[Cp^*Rh][(COD)Co]$-$[Se_2C_2(B_{10}H_{10})]$ (**25b**). However, the same reaction with $Cp^*Co[S_2C_2(B_{10}H_{10})]$ leads to $[Cp^*Rh][(COD)Co][S_2C_2(B_{10}H_{10})]$ (**26a**) as an open caged species (Scheme 5). The Rh–Co bond lengths in **25** and **26** are 2.63 and 2.71 Å respectively. The different reaction pathways arise from the slight difference in the electronic properties of S and Se. Other main products isolated in both reactions include the complexes **4a**/**b**.

Synthesis of the hetero-bimetallic Rh–Co complex $[Cp^*Rh][(COD)Co][E_2C_2(B_{10}H_{10})]$ (**27a**/**b**) uses the reactions of $(Cp^*Rh)[E_2C_2(B_{10}H_{10})]$ with $CpCo(CO)_2$ or $CpCo(C_2H_4)_2$ in the presence of Me_3NO, taking advantage of carbonyl and ethylene as good leaving groups [18]. The Rh–Co distance for **27a** and **27b** are 2.48 and 2.51 Å respectively, suggesting stronger metal–metal bonding interactions relative to **25b** and **26a** [14] (Scheme 6).

Theoretical studies of the MO orbitals in the binuclear complexes **27b** provide some insight into the bonding (Fig. 3). From the picture of molecular orbitals, strong interactions between the two metal centers (contributed mostly from the s, p_y and d orbitals of rhodium and cobalt) are in accordance with the assistance of the selenium atoms (s contribution). Natural Bond Orbital (NBO) analysis shows a polar covalent bond between the two metals, with 41% contribution of Rh (with sd hybrid orbitals) and 59% of Co (with d orbitals).

A similar approach is also successful for the synthesis of binuclear Ir–Rh complexes using $(Cp^*Ir)[E_2C_2(B_{10}H_{10})]$ as precursors. Allowing them to react with low-oxidation-state rhodium complexes leads to various fascinating complexes with B–B and B–H activations. (Scheme 7). Thus, reaction of 2 equiv. of $Cp^*Ir[S_2C_2(B_{10}H_{10})]$ with $[(COD)Rh(\mu\text{-}OCH_3)]_2$ in a boiling toluene/methanol mixture affords the bimetallic $[Cp^*Ir][(COD)Rh][S_2C_2(B_{10}H_9)]$ (**28a**) in 32% yield, $[Cp^*Ir][(COD)Rh][S_2C_2(B_{10}H_{10})]$ (**29a**) in 10% yield and $[Cp^*Ir][(COD)Rh](OCH_3)[S_2C_2(B_9H_9)]$ (**30a**) in 41% yield. Note that **28a** is a cyclometallic complex with a direct Ir–B interaction (2.096 Å) but **29a** only shows the trend of B–H activation. These two products appear to arise from the competition of B–H activation induced by different metallic sites where iridium is a more effective inducer than rhodium. This assumption is also confirmed by the structure of **30a**, which probably arises from the iridium induced cage opening at B3 followed by a B–H activation at B6. The different configuration of **28a**, **29a** and **30a** also provide models for the more general B–B and B–H activation with iridium. In another route to form Rh–Ir bonds, $[Rh(COD)(\mu\text{-}Cl)]_2$ seems to be a less active reagent than $[Rh(COD)(\mu\text{-}OCH_3)]_2$ and **28a** is obtained as the only

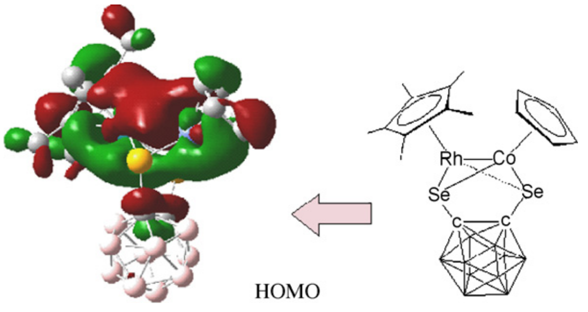

Fig. 3. HOMO of complex **27b**.

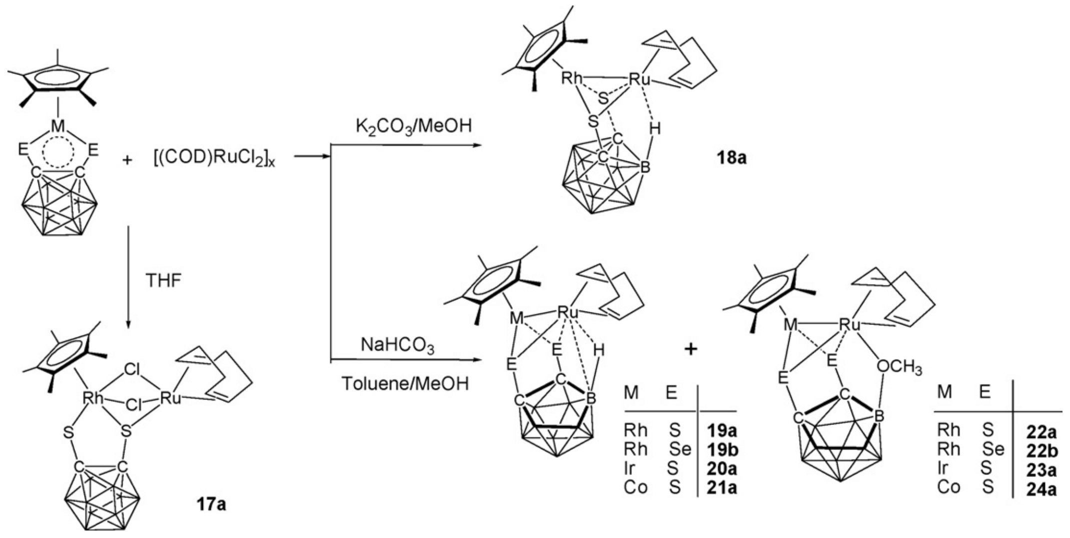

Scheme 4. Syntheses of Ru–Co/Rh/Ir binuclear complexes.

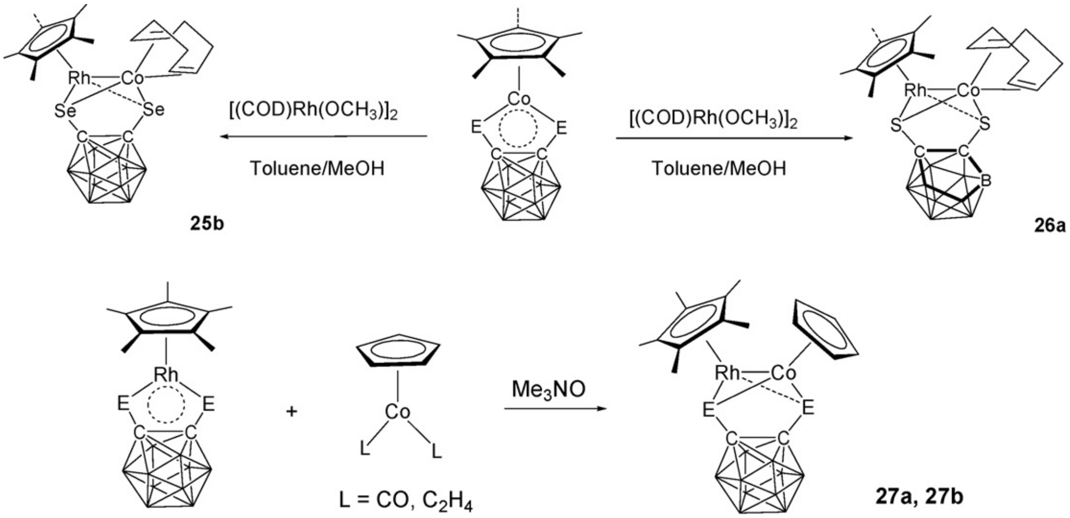

Scheme 5. Syntheses of Rh–Co binuclear complexes.

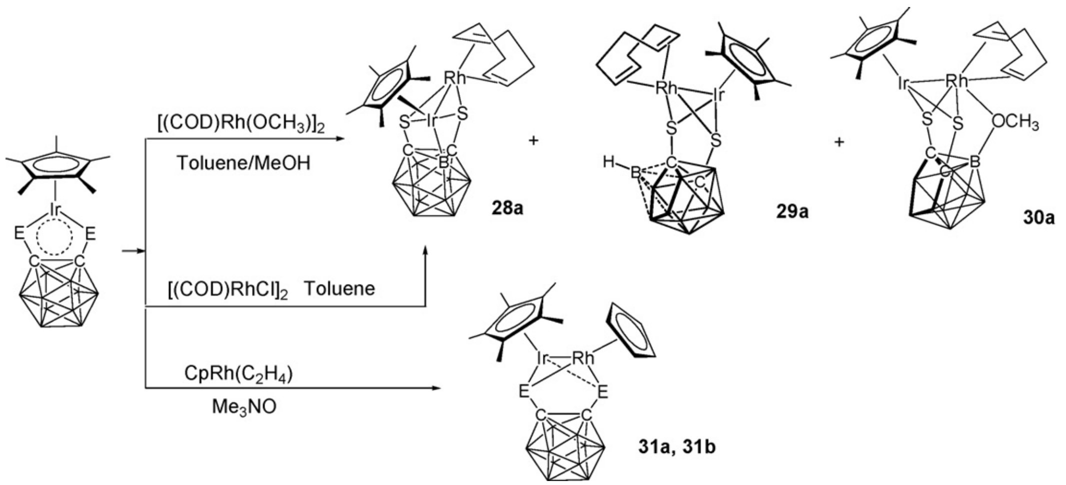

Scheme 6. Syntheses of Rh–Ir binuclear complexes.

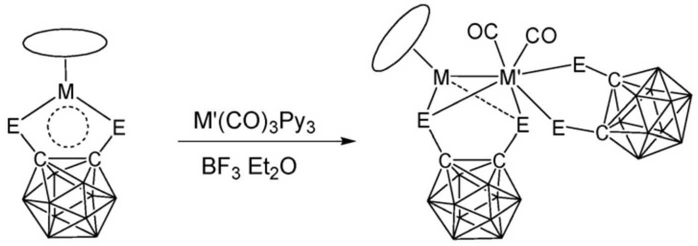

M	M'	⬭	
Co	Mo	Cp*	**32a, 32b**
Co	W	Cp*	**33a, 33b**
Co	W	Cp^{tt}	**34a, 34b**
Co	W	Cp	**35a, 35b**
Rh	Mo	Cp*	**36a, 36b**
Rh	W	Cp*	**37a, 37b**
Rh	Mo	Cp^{tt}	**38a, 38b**
Rh	W	Cp^{tt}	**39a, 39b**

Scheme 7. Syntheses of Rh/Co–Mo/W binuclear complexes.

product [15]. The reaction with $CpRh(C_2H_4)_2$ is quite similar to that used for the formation of heterometallic Rh–Co bonds. The resulting product is shown to be a simple binuclear complex with a short Ir–Rh distance of 2.64 Å (**31a**). Unfortunately, the reactions of low oxidation state iridium complexes with $(Cp^*Rh)[E_2C_2(B_{10}H_{10})]$ are found to be too complicated and sensitive.

2.2.4. Formation of Rh/Co-Mo/W bonds

The reactions between the 16-electron precursors of Co, Rh, Ir, Ru and group 6 metal complexes $M(CO)_3(py)_3$ (M = Mo, W) (py = pyridine, NC_5H_5) are simpler and cleaner compared with the homo- and hetero-binuclear products of group 8 and group 9 metals. The construction of the M–M bonds between group 9 metals and Mo/W seems to be more accessible. Thus $\{Cp^{\#}M[E_2C_2(B_{10}H_{10})]\}\{M'(CO)_2[E_2C_2(B_{10}H_{10})]\}$ (M = Co, Rh; M′ = Mo, W) containing direct metal–metal interactions can be isolated but only in relatively low yield (**32a/b**–**39a/b** in Scheme 7). In general, the combinations of $M(CO)_3(py)_3$ and BF_3 are found to be effective ways to generate reactive $[M'(CO)_3]$ fragments, for insertion into the electron deficient half-sandwich precursors. The final bi- and trimetallic products are formed under the association of 1,2-dicarba-*closo*-dodecarborane-1, 2-dichalcogenolates [18–20].

The Co–W (2.65–2.71 Å), Rh–W (around 2.75 Å), Co–Mo (2.63 Å), and Rh–Mo (2.76–2.83 Å) distances are all in the range of metal–metal single bonds obtained by X-ray single crystal analysis. All of the bimetallic complexes exhibit similar structures and configurations, containing two *o*-carboranedichalcogenate ligands. One of these *o*-carboranedichalcogenate ligands serves as a bridging ligand whereas the other is attached only to the $[M'(CO)_2]$ fragments. The Mo and W atoms exhibit seven-coordinate geometry with two terminal carbonyls.

Another Co–W bimetallic complex **46b** ($[\{CpCo(Se_2C_6H_4)\}(Se_2C_6H_4)W(CO)_2]$) is obtained from reaction of $[CpCo(Se_2C_6H_4)]$ with 1 equiv. of $[W(CO)_3(py)_3]$ in the presence of more than 10 equiv. of $BF_3\ OEt_2$ in diethyl ether under reflux. The configuration of **46b** is similar to **32a/b** and **33a/b**. The Co–W bond length is 2.62 Å, which is a little shorter than that in complexes **32** and **33** [7].

2.2.5. Formation of Co/Rh/Ir–Fe bonds

Although attempts to prepare 16-electron precursors $Cp^{\#}Fe[E_2C_2(B_{10}H_{10})]$ do not lead to successful product isolations, iron can still be successfully introduced into the systems through the formation of Co–Fe [21], Rh–Fe [21] and Ir–Fe [22] bonds. The electron rich $Fe(CO)_5$ is chosen for the reactions with the 16-electron precursors of group 9 metals (Scheme 8). Reactions of $Cp^{\#}M[E_2C_2(B_{10}H_{10})]$ (M = Co, Rh, Ir) with $Fe(CO)_5$ in the presence of 2 equiv. of Me_3NO afford the complexes $\{Cp^{\#}M[E_2C_2(B_{10}H_{10})]\}Fe(CO)_3$ (M = Co, Rh, Ir; **41a/b**–**46a/b**) in 20–50% yields. Both the group 9 metals and iron are six-coordinate. Direct M–Fe interactions are observed and the $[Cp^{\#}M]$ and $[Fe(CO)_3]$ units are bridged by two μ-chalcogen atoms from the bridging carboranyl ligands. The bond lengths are 2.40–2.42 Å (Co–Fe), 2.51–2.55 Å (Rh–Fe) and 2.58 Å (Ir–Fe) respectively, in the range for single bonds [16,17].

Similar reactions have been reported by Nishihara et al. Thus treatment of $[CoCp(S_2C_6H_4)]$ with 1 equiv. of $Fe(CO)_5$ and 2 equiv. of Me_3NO in toluene affords a dinuclear complex $[CpCo(S_2C_6H_4)Fe(CO)_3]$ (**47a**). The Co–Fe bond length is 2.42 Å, in accord with **41a** and **42a** [7].

2.3. Trinuclear complexes with metal–metal bonds

2.3.1. Formation of M–Mo/W–M (M = Co, Rh, Ir) bonds

Multinuclear complexes in the form of M–M′–M can be synthesized by reactions of the 16-electron precursors with $M(CO)_3(py)_3$ (M = Mo, Co). In addition to the asymmetric binuclear complexes (**32a/b**–**39a/b**) the trimetallic complexes $\{Cp^{\#}M_2[E_2C_2(B_{10}H_{10})]_2\}M'(CO)_2$ (M = Mo, W; M′ = Co, Rh, Ir) (**48a/b**–**53a/b**) are always isolated as main products from the same reactions [16,17] (Scheme 9). In a typical structure two group 9 metals are connected by a molybdenum or tungsten dicarbonyl unit. Supported by a symmetric bridging ortho-carborane-1,2-diselenolato ligand, the Co–Mo/W, Rh–Mo/W bonds consist with the bimetallic complexes **41a/b**–**46a/b**, while the distances of Ir–Mo are around 2.78–2.82 Å, and Ir–W is about 2.79 Å, lying in the range of single bonds [14,15].

Analysis of the bonding in **52a** suggests a complicated situation involving the three metals. Thus HOMO−1 is apparently a bonding orbital with contributions from the p_x and d orbitals of two iridium atoms, the d orbitals of molybdenum, and the s and p_z orbitals of the sulfur atoms. However, the HOMO shows distinct antibonding character in the Ir–Mo–Ir chain, suggesting weakening of the metal–metal bonds. Meanwhile, strong bridging orbital distributions derived from the sp orbitals of the sulfur atoms hold the molecule together (Fig. 4). This confirms that the 1,2-dicarba-*closo*-dodecarborane-1,2-dichalcogenolates play a significant role as a non-innocent ancillary ligand.

The clusters $[\{CpM(S_2C_6H_4)\}_2Mo(CO)_2]$ (M = Co, Rh) (**54a/b**, **55a/b**, **56a**) can be formed from reaction of the dithiolene complex $[CpCo(S_2C_6H_4)]$ or $[CpRh(S_2C_6H_4)]$ with $[Mo(CO)_3(py)_3]$ in the presence of $BF_3\ OEt_2$. The Mo–Co distances are 2.63 Å and the Mo–Rh distances are 2.72–2.76 Å, which lie in the usual range for single bonds [8,9].

2.3.2. Formation of M–Ni–M (M = Co, Rh) bonds

The low-valent nickel reagent $Ni(COD)_2$ can be used to form Co/Rh–Ni bonds. Thus, reactions of $Ni(COD)_2$ with 2 equiv.

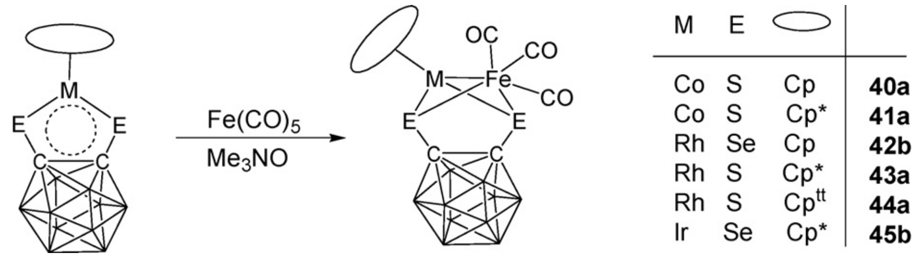

Scheme 8. Syntheses of Co/Rh/Ir–Fe binuclear complexes.

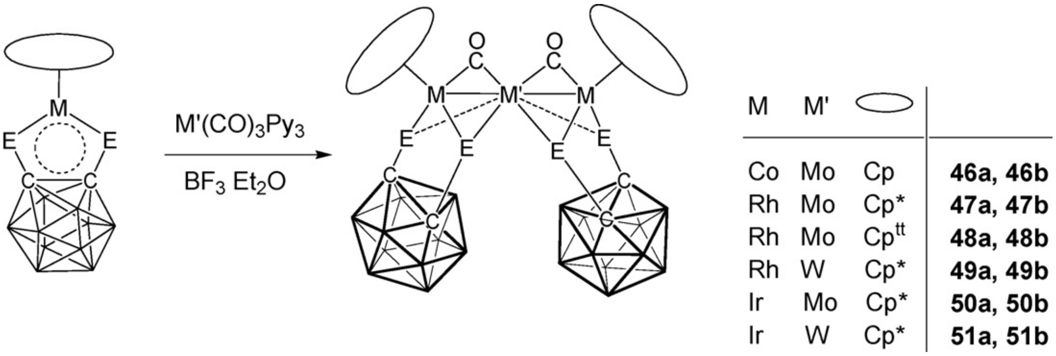

Scheme 9. Syntheses of M–Mo/W–M (M = Co, Rh, Ir) trinuclear complexes.

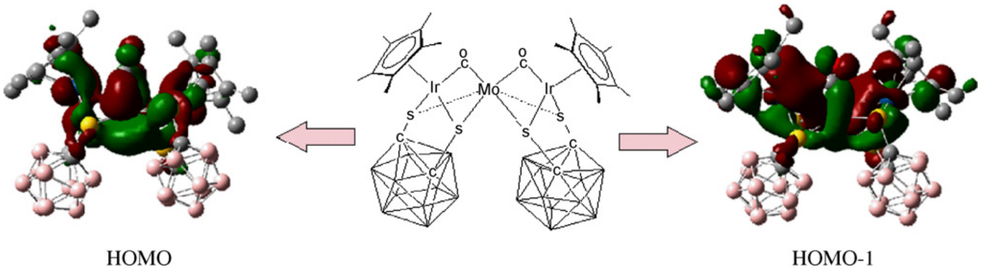

Fig. 4. Frontier orbitals of complex **52a**.

of $Cp^{\#}M[E_2C_2(B_{10}H_{10})]$ (M = Co, Rh) in toluene afford heterotrinuclear complexes $\{CpM[E_2C_2(B_{10}H_{10})]\}_2Ni$ (**57a**, **58a**, **58b**) in about 30–50% yield (Scheme 10). The single bonds are about 2.36–2.37 Å for Co–Ni [23] and about 2.46–2.49 Å for Rh–Ni [24]. Most of these complexes are air and moisture sensitive. In reactions with half-sandwich iridium precursors, stable clusters are isolated containing chloride bridges between Ir and Ni without any direct metal–metal interactions.

2.3.3. *Formation of M–Co–Co (M = Co, Rh, Ir) bonds*

Another type of trimetallic clusters contains M–Co–Co triangles. Thus, reactions of the group 9 precursors $Cp^{\#}M[E_2C_2(B_{10}H_{10})]$ (M = Co, Rh, Ir) with $Co_2(CO)_8$ in a 1:1 molar ratio at room temperature are rapid and complete. The crystallized products, $Cp^{\#}Co[E_2C_2(B_{10}H_{10})][Co_2(CO)_5]$ (**59a/b**, **60a/b**) [23], $[Cp^{\#}Rh\{E_2C_2(B_{10}H_{10})\}][Co_2(CO)_5]$ (**61a/b**, **62a/b**) [20] and $[Cp^{\#}Ir\{E_2C_2(B_{10}H_{10})\}][Co_2(CO)_5]$ (**63a/b**, **64a/b**) [22], can be isolated by chromatography on silica gel in about 70% yield (Scheme 11). The yields are even higher in the presence of the decarbonylation reagent Me_3NO. All of the products are neutral, diamagnetic, and air-sensitive in solution. The Co–Co distances are around 2.44–2.45 Å, and the M–Co distances are 2.55–2.59 Å (Co–Co), 2.61–2.66 Å (Rh–Co) and 2.60–2.65 Å (Ir–Co), indicating strong interactions between the metals.

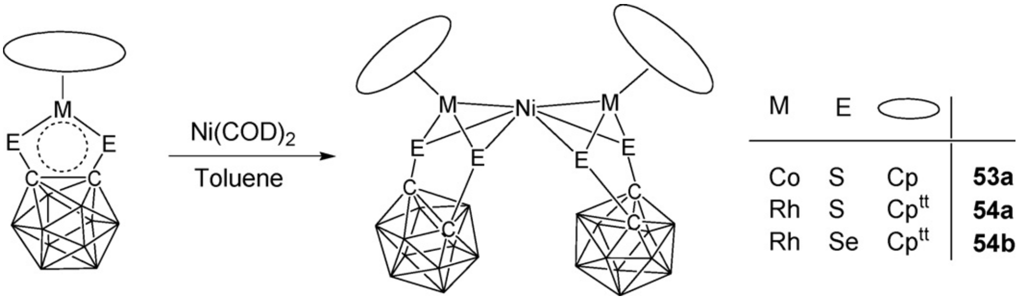

Scheme 10. Syntheses of M–Ni–M (M = Co, Rh, Ir) trinuclear complexes.

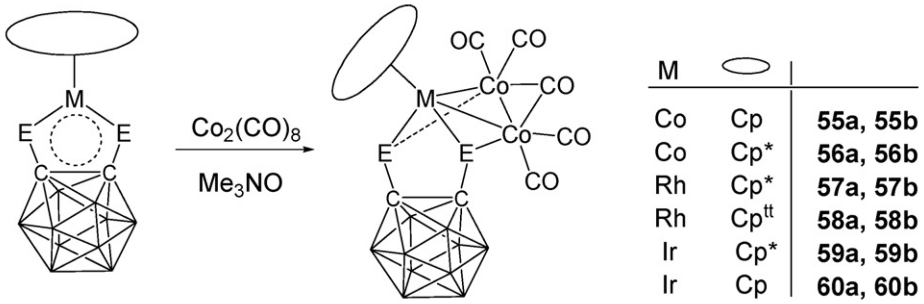

Scheme 11. Syntheses of triangle M–Co–Co complexes.

Similarly, the trinuclear heterometallic complexes $[\{Cp^*M(S_2C_6H_4)\}Co_2(CO)_5]$ (M = Rh, Ir, Ru) (**65a**–**67a**) can be synthesized from mononuclear metalladithiolene precursors $[MCp(S_2C_6H_4)]$ (M = Rh, Ir, Ru), respectively. The planarity of the metalladithiolene ring is maintained in these complexes which are different from the previous trinuclear complexes. The average Co–M distances in these complexes is 2.61 Å (Co–Rh), 2.61 Å (Co–Ir), and 2.62 Å (Co–Ru), respectively [10].

2.3.4. Homo- and hetero-metallic tri- and tetra-nuclear complexes with Ir, Rh and Ru

Reactions of the low oxidation state Rh and Ir reagents appear to be more complicated and lead to products exhibiting B–H activation and open cages. By controlling the reaction conditions, a series of trimetallic clusters containing Rh, Ir and Ru have been synthesized from such reactions. Normally, controlling the mole ratio of two reactants and using non-proton solvent are convenient

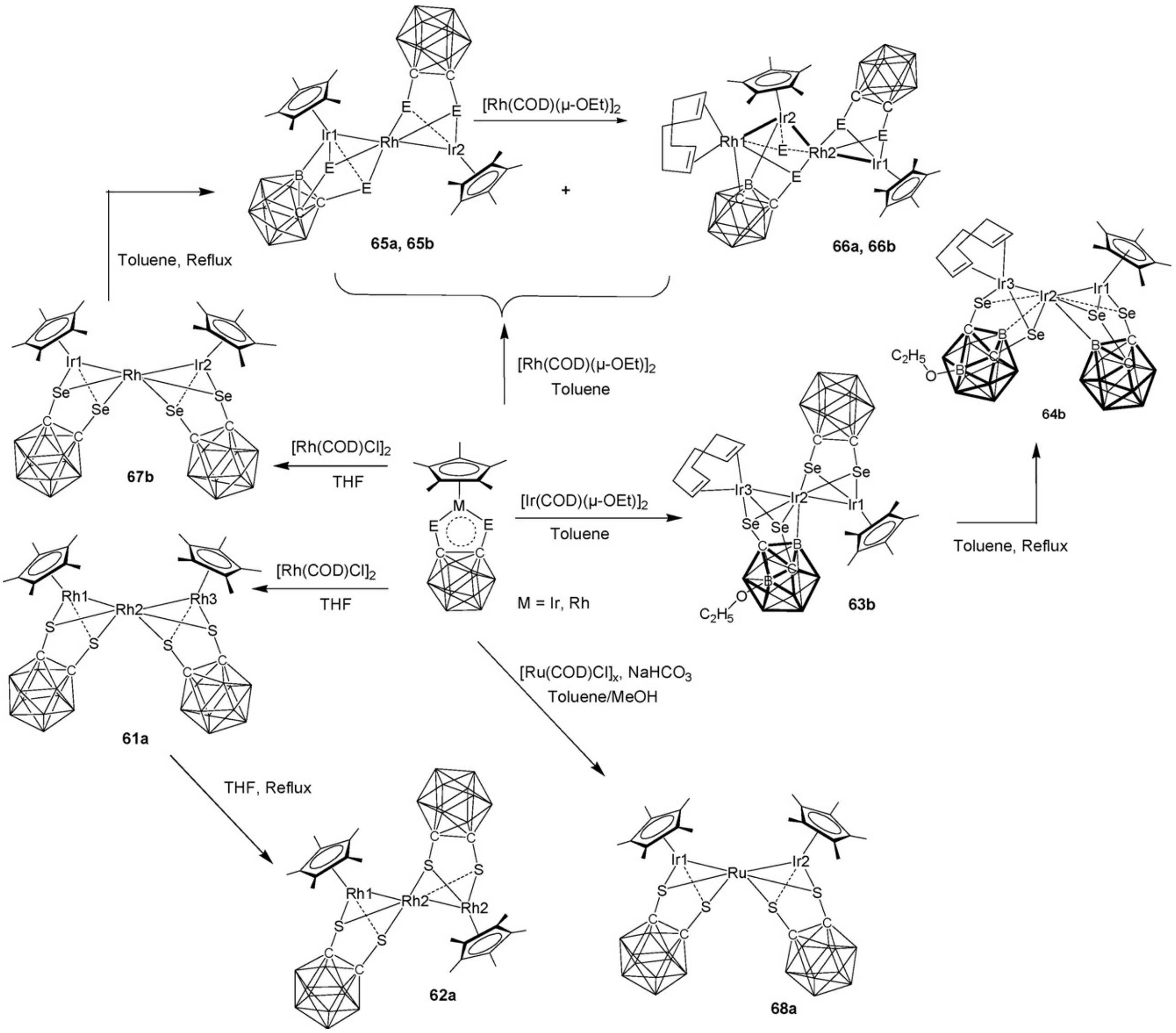

Scheme 12. Syntheses of trinuclear complexes with Ir, Rh and Ru.

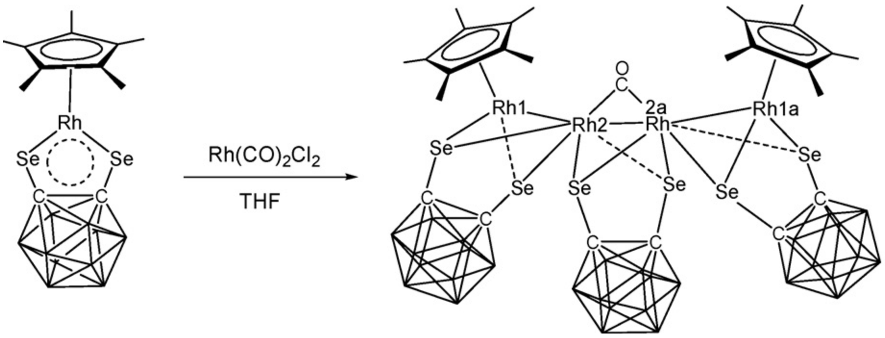

69b

Scheme 13. Synthesis of tetranuclear complex.

ways to achieve those products without carborane cage opening (Scheme 12).

Homo-trinuclear rhodium and iridium complexes can be prepared from the reactions of 16-electron precursors with suitable metal reagents in THF. Thus *cis*-[{Cp*Rh[S$_2$C$_2$(B$_{10}$H$_{10}$)]}$_2$Rh] (**68a**) and *trans*-[{Cp*Rh[S$_2$C$_2$(B$_{10}$H$_{10}$)]}$_2$Rh] (**69a**) are synthesized from [Rh(COD)(μ-Cl)]$_2$ and 2 equiv. of Cp*Rh[S$_2$C$_2$(B$_{10}$H$_{10}$)] in 25% and 39% yields respectively [26]. When heated in boiling THF, *cis*-**68a** can be converted to the *trans*-isomer **69a** in more than 95% yield, indicating that *trans*-**69a** is the thermodynamically stable product. Both of these products have been isolated and characterized by X-ray crystal structure determination. Complex **68a** has a symmetric configuration containing a C_2 axis and with a Rh–Rh bond length of 2.65 Å. In the stereoisomer **69a**, the *o*-carborane groups are drawn close to the rhodium center with a Rh–B distance of 3.16 Å (3.38 Å in **69a**). The Rh–Rh distance increases to 2.82 Å.

The syntheses of tri-iridium clusters also start from 2 equiv. of Cp*Ir[S$_2$C$_2$(B$_{10}$H$_{10}$)] and [Ir(COD)(μ-Cl)]$_2$ in toluene. However, the yield of this reaction is very low. However, by using the more reactive reagent [Ir(COD)(μ-OC$_2$H$_5$)]$_2$, the two expected complexes are isolated as *cis*-**71b** and *trans*-**70b** [27]. X-ray single crystal analysis demonstrates that **70b** is an asymmetric complex containing a (COD)Ir fragment and a Cp*Ir fragment bridged by the third iridium atom. The Ir1–Ir2 bond length is 3.17 Å, which is much longer than the Ir1–Ir3 bond length of 2.73 Å. This can be explained by the different oxidation states of Ir1$^{\mathrm{III}}$ and Ir2$^{\mathrm{II}}$. In addition, one side of the bridging carborane ligand exhibits strong B–H activation, where B3 is directly bonded to Ir1 and B6 is functionalized by an ethoxy group. Heating **70b** in boiling toluene affords **71b** in 90% yields as a *cis*-isomer, implying different relative thermodynamic stabilities than **68a**/**69a**. A further B–H activation accompanies the stereoisomerization in the transformation of **70b** to **71b**. The B3 on the other side of carborane ligand becomes bonded to the iridium atom. The Ir1–Ir3 and Ir1–Ir2 bonds are lengthened to 2.91 and 3.13 Å, respectively.

The reactions of Cp*Ir[Se$_2$C$_2$(B$_{10}$H$_{10}$)] with 1 equiv. of the rhodium reagent afford hetero-binuclear Ir–Rh complexes. However, a trimetallic Ir–Rh–Ir bonding complex is obtained when more than 2 equiv. of the iridium reagent is used. In the reactions of the precursors with [Rh(COD)(μ-Cl)]$_2$ in THF, the *cis*-**74b** and *trans*-**72a/b** are observed and isolated in moderate yields [25,26]. Complex **74b** can be changed into **72b** when heated in boiling toluene. The structure of **72b** is similar to that of **69a** except that one of the ancillary *o*-carborane ligands is linked to an iridium atom through an Ir–B interaction. The Ir1–Rh1 bond (3.00 Å) is longer than the Ir2–Rh1 bond (2.69 Å).

A similar reaction of Cp*Ir[S$_2$C$_2$(B$_{10}$H$_{10}$)] with [Ru(COD)(μ-Cl)]$_x$ leads to a similar *cis*-[{Cp*Ir[S$_2$C$_2$(B$_{10}$H$_{10}$)]}$_2$Ru] (**75a**) product. Both the bimetallic complexes **20a** and **23a** and the trimetallic **75a** can be separated by chromatography. The structure of **75a** shows the same Ir–B distance of 2.71 Å with neither B–H activation nor cage opening on either carborane unit.

Reaction between [Rh(COD)(μ-OC$_2$H$_5$)]$_2$ and Cp*Ir[S$_2$C$_2$(B$_{10}$H$_{10}$)] in a 1:2 mole ratio leads to the unexpected formation of both tri- and tetra-nuclear complexes (**72a/b**, **73a/b**), which can be isolated after chromatography in 18% and 30% yield, respectively [26,28]. The structure of **73a/b** shows three short intermetallic separations which lie in the expected range of a single bond, namely 2.60 Å for Ir1–Rh2, 2.98 Å for Rh2–Ir2, and 2.78 Å for Ir2–Rh1. The two dithiolato ligands of the carboranes are situated at the both sides of the tetrametallic plane with three of the chalcogen atoms acting as bridging ligands and a fourth chalcogen atom bonded to three metals. All of the metal atoms are in different coordination environments. The Ir2, Rh1 and Rh2 atoms all exhibit six-coordinate geometry while Ir1 is only five-coordinate. One side of the carborane ligand exhibits a variety of bonding modes, namely one Ir–B bond derived from B–H activation, one Rh–C bond formed probably by C–S bond cleavage and another C–S–Rh bond remaining from the 16-electron half-sandwich precursor. Thus the complexes **73a**/**b** are very complicated species, which can also arise from the reactions of **72a/b** with [Rh(COD)(μ-OC$_2$H$_5$)]$_2$ in toluene in moderate yield [28]. The study of this reaction provides a potential method to synthesize organometallic clusters containing more than four metal atoms.

Another tetranuclear complex with metal–metal bonding (Cp*Rh)$_2$Rh$_2$(CO)[Se$_2$C$_2$(B$_{10}$H$_{10}$)]$_3$ (**76b**) is obtained from the reaction of Cp*Rh[Se$_2$C$_2$(B$_{10}$H$_{10}$)] with Rh(CO)$_2$Cl$_2$ in a 1:1 mole ratio (Scheme 13). Compared with the unsymmetrical complexes **73a/b** and **76b** crystallizes in a high symmetric tetragonal crystal system. Four rhodium atoms are contained in one molecule with bond lengths of 2.66 Å between Rh1 and Rh2, and 2.68 Å between Rh2 and Rh2a. Three dithiolate carborane ligands bridge each of two Rh atoms and one carbonyl group bridges Rh2 and Rh2a.

3. Applications of multimetallic clusters

The 16-electron carborane–dichalcogenolate complexes are promising precursors for the synthesis of multinuclear transition metal clusters because of the mild reaction conditions, diverse product types, and facile product characterization. Some efforts have been made in the exploration of special optical and physical properties of the increasing variety of available multimetallic complexes. Nonlinear optical materials are of particularly interest, since they have potential applications in the protection of optical sensors from high-intensity laser beams because of the special transmission features under different light intensity. Fullerenes (C$_{60}$) and dithiolene metal complexes are generally regarded as the best substances for nonlinear optical properties.

The trinuclear cluster **50a** with Ir–Mo–Ir interactions was chosen for an initial investigation of nonlinear optical properties because of its stability and the high yield in its synthesis. The third-order NLO determinations were carried out using the Z-scan measurements method with a 532 nm laser. The normalized transmittance of **50a** drops to about 73% at the focus, and the corresponding third-order NLO absorptive coefficient α^2 is 2.27×10^{-10} m/W. This is an improvement over the metal clusters, ferrocene derivatives, and coordination polymers exhibiting NLO properties. The effective third-order refractive index n_2 is calculated to be 6.84×10^{-11} esu. The calculated c value for **50a** is 2.60×10^{-29} esu, which is several orders of magnitude larger than those in well known as NLO material (5.6×10^{-35}–8.6×10^{-34} esu for group 10 metal alkynyl polymers at 1064 nm and 7.5×10^{-34} esu for C_{60} at 1910 nm) [29]. This recent discovery of outstanding nonlinear optical properties of **50a** suggests considerable potential for optical applications using rationally designed heteronuclear organometallic clusters.

4. Conclusion

A facile strategy to construct M–M bonds between late transition metals with $[E_2C_2(B_{10}H_{10})]^{2-}$ and $(E_2C_6H_4)^{2-}$ as ancillary ligands is reviewed. Thus reactions of the 16-electron precursors with low-valent organometallic reagents lead to redox reactions between the transition metal centers in the two reactants. As a result, the group 9 metals in $Cp^{\#}M[E_2C_2(B_{10}H_{10})]$ and $Cp^{\#}M(E_2C_6H_4)$ are reduced from M^{III} to M^{II} by the low oxidation state metal reagents leading to stable M–M interactions accompanied by the bridging ligands. Theoretical studies of such multinuclear complexes reveal the electronic features of the 16-electron precursors. The electron deficient metal centers and the empty p orbitals along the *z* axis of the chalcogens make these precursors very useful for constructing M–M bonds. The M–M bonding in the complexes appears to be complicated according to the MO and NBO analysis. Thus most of the M–M bonds are covalent polar bonds with d contributions from both metals. In addition, the iridium species bearing 1,2-dicarba-*closo*-dodecarborane-1,2-dichalcogenolate ligands frequently undergo activation of B–B and B–H bonds, probably because of the large size and flexibility of the iridium atom. Compared with the complexes bearing 1,2-dicarba-*closo*-dodecarborane-1,2-dichalcogenolates ligands, the reactions of the 16-electron complexes $[MCp(S_2C_6H_4)]$ are less developed. However, there are some advantages which make the precursor unique and promising. For example, multiple substitution on benzene can give two or even three electron deficient centers in a single complex, which can facilitate the construction of cyclic heterometalladithiolene clusters via M–M bond formation [11]. These achievements are also highlighted by the possibilities of their promising applications in nonlinear optical properties as well as other special optical and physical properties currently under investigation.

Acknowledgments

This work was supported by the National Science Foundation of China (20531020, 20721063, and 20771028), Shanghai Science and Technology Committee (08DZ2270500 and 08DJ1400103), Shanghai Leading Academic Discipline Project (B108) and the National Basic Research Program of China (2009CB825300).

References

[1] (a) R.H. Crabtree, The Organometallic Chemistry of the Transition Metals: 4th ed., Wiley InterScience, 2005;
(b) L.H. Gade, Angew. Chem. Int. Ed. 39 (2000) 2658;
(c) B. Bosnich, Inorg. Chem. 38 (11) (1999) 2554;
(d) E.K. Van den Beuken, B.L. Feringa, Tetrahedron 54 (1998) 12985;
(e) H.T. Chifotides, K.R. Dunbar, Acc. Chem. Res. 38 (2005) 146;
(f) S. Liu, Y.F. Han, G.-X. Jin, Chem. Soc. Rev. 36 (2007) 1543;
(g) S. Liu, G.-L. Wang, G.-X. Jin, Dalton Trans. (2008) 413.
[2] M.C. Comstock, J.R. Shapley, Coord. Chem. Rev. 143 (1995) 501.
[3] G.-X. Jin, Coord. Chem. Rev. 248 (2004) 587.
[4] M. Herberhold, G.-X. Jin, H. Yan, W. Milius, J. Organomet. Chem. 587 (1999) 252.
[5] S.X. Lu, G.-X. Jin, S. Eibl, M. Herberhold, Y. Xin, Organometallics 21 (2002) 2533.
[6] J.Q. Wang, L.H. Weng, G.-X. Jin, Rev. Inorg. Chem. 25 (2005) 55.
[7] N. Nakagawa, T. Yamada, M. Murata, M. Sugimoto, H. Nishihara, Inorg. Chem. 45 (2006) 14.
[8] M. Nihei, T. Nankawa, M. Kurihara, H. Nishihara, Angew. Chem. Int. Ed. 38 (1999) 1098.
[9] S. Muratsugu, K. Sodeyama, F. Kitamura, M. Sugimoto, S. Tsuneyuki, S. Miyashita, T. Kato, H. Nishihara, J. Am. Chem. Soc. 131 (2009) 1388.
[10] M. Murata, S. Habe, S. Araki, K. Namiki, T. Yamada, N. Nakagawa, M. Nihei, J. Mizutani, M. Kurihara, H. Nishihara, Inorg. Chem. 45 (2006) 1108.
[11] B.-H. Zhu, Y. Shibata, S. Muratsugu, Y. Yamanoi, H. Nishihara, Angew. Chem. Int. Ed. 48 (2009) 3858.
[12] S.Y. Cai, X.F. Hou, L.H. Weng, G.-X. Jin, J. Organomet. Chem. 690 (2005) 910.
[13] D.H. Kim, J. Ko, K. Park, S. Cho, S.O. Kang, Organometallics 18 (1999) 2738.
[14] S. Liu, G.-X. Jin, Dalton Trans. (2007) 949.
[15] J.Q. Wang, M. Herberhold, G.-X. Jin, Organometallics 25 (2006) 3508.
[16] Y.Q. Chen, J.Q. Wang, G.-X. Jin, J. Organomet. Chem. 692 (2007) 5190.
[17] J.-S. Zhang, Y.-J. Lin, Jin S G.-X., Dalton Trans. (2009) 111.
[18] W. Li, L.H. Weng, G.-X. Jin, Inorg. Chem. Commun. 7 (2004) 1174.
[19] S.Y. Cai, Y.J. Lin, G.-X. Jin, Dalton Trans. (2006) 912.
[20] S.Y. Cai, G.-X. Jin, Organometallics 24 (2005) 5280.
[21] S.Y. Cai, X.F. Hou, Y.Q. Chen, G.-X. Jin, Dalton Trans. (2006) 3736.
[22] J.Q. Wang, X.F. Hou, L.H. Weng, G.-X. Jin, Organometallics 24 (2005) 826.
[23] Y.Q. Chen, J.S. Zhang, S.Y. Cai, X.F. Hou, H. Schumann, G.-X. Jin, Dalton Trans. (2007) 749.
[24] S.Y. Cai, J.Q. Wang, G.-X. Jin, Organometallics 24 (2005) 4226.
[25] G.-X. Jin, J.Q. Wang, C. Zhang, L.H. Weng, M. Herberhold, Angew. Chem. Int. Ed. 44 (2005) 259.
[26] J.Q. Wang, S.Y. Cai, G.-X. Jin, L.H. Weng, M. Herberhold, Chem. Eur. J. 11 (2005) 7342.
[27] S. Liu, J.Q. Wang, L.H. Weng, G.-X. Jin, Dalton Trans. (2007) 3792.
[28] G.-X. Jin, J.Q. Wang, Dalton Trans. 1 (2006) 86.
[29] J.Q. Wang, G.-X. Jin, Inorg. Chem. Commun. 10 (2007) 463.